AIAA Paper No. 69-67

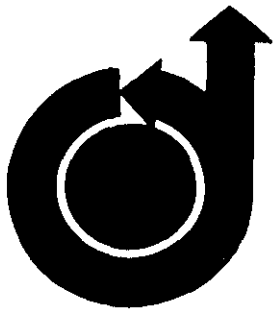

AN EXPERIMENTAL STUDY OF THE NEAR WAKE OF A TWO-DIMENSIONAL HYPERSONIC BLUNT BODY WITH MASS ADDITION

by

DONALD J. COLLINS, LESTER LEES
and
ANATOL ROSHKO
California Institute of Technology
Pasadena, California

AIAA 7th Aerospace Sciences Meeting

NEW YORK CITY, NEW YORK/JANUARY 20-22, 1969

AN EXPERIMENTAL STUDY OF THE NEAR WAKE OF A TWO-DIMENSIONAL HYPERSONIC BLUNT BODY WITH MASS ADDITION*

Donald J. Collins, Lester Lees, Anatol Roshko
California Institute of Technology
Pasadena, California

Abstract

An experimental investigation of the steady, laminar near-wake flow field of a two-dimensional, adiabatic, circular cylinder with surface mass transfer has been made at a free-stream Mach number of 6.0. The pressure and mass-concentration fields associated with the transfer of argon, nitrogen or helium into the near wake were studied for mass transfer from the forward stagnation region, and from the base. For sufficiently low mass transfer rates from the base, for which a recirculating zone exists, the entire near-wake flow field correlates with the momentum flux, not the mass flux, of the injectant, and the mass-concentration field is determined by counter-current diffusion into the reversed flow. For mass addition from the forward stagnation region, the pressure field is undisturbed and the mass-concentration field is nearly uniform in the region of reversed flow. The axial decay of argon mass concentration in the intermediate wake, downstream of the neck, is explained with the aid of an integral solution in the incompressible plane, from which the location of the virtual origin for the asymptotic far-wake solution has been derived as one result.

List of Symbols

C_∞ $\frac{\mu}{\mu_\infty}\frac{T_\infty}{T}$ - Chapman-Rubesin factor

C, C_i ρ_i/ρ - mass concentration

d cylinder diameter

D binary diffusion coefficient

$G(M_\infty)$ $\frac{P_0}{P_\infty}\frac{1}{M_\infty}\left[\frac{T_\infty}{T_0}\right]^{\frac{1}{2}} = \frac{1}{M_\infty}\left[1+\frac{\gamma-1}{2}M_\infty^2\right]^{\frac{\gamma+1}{2(\gamma-1)}}$

H $\frac{\dot m_i}{\dot m_f}G(M_\infty)$ - Korst injection parameter

I $\frac{\dot m_i}{2\dot m_{B.L.}}\left[\frac{m_{Air}}{m_i}\right]^{\frac{1}{2}}$ - mass transfer parameter

$\dot m_{B.L.}$ $\left[\int_0^\delta \rho u\,dy\right]_s = \rho_e u_e(\delta-\delta^*)$ - mass flux per unit span in cylinder boundary layer upstream of separation

$\dot m_f$ $\rho_\infty u_\infty d$ - intercepted free-stream mass flux per unit span

$\dot m_i$ mass flux per unit span of injectant

$\dot M$ $\frac{\dot m_i}{2\dot m_{B.L.}}$ - mass transfer parameter

M Mach number

m molecular weight

P pressure

P_{0_2} Pitot pressure, impact pressure

$Re_{\infty,d}$ $\frac{u_\infty d}{\nu_\infty}$, Re_x $\frac{u_e x}{\nu_e}$ } Reynolds numbers

Sc $\frac{\nu}{D}$ - Schmidt number

T temperature

u, v physical velocity components

u^* $\frac{u_{\psi=0}}{u_e}$ - dividing streamline velocity ratio

U u/u_e - transformed velocity

$\tilde U(\tilde X)$ $\frac{u(\tilde X)}{u_{max}}\cdot\frac{|u_{max}|(x_r-x_b)}{D} = Re(\tilde X)Sc$

x, y physical coordinates

$\tilde X$ $\frac{x-x_b}{x_r-x_b}$ - transformed physical x

X $\int_0^{x/d}\frac{\rho_e u_e \mu_e}{\rho_\infty u_\infty \mu_\infty}\,d(x/d)$ - modified Howarth coordinate

x_r location of reattachment

$\tilde Y$ $\frac{y}{x_r-x_b}$ - transformed physical y

Y $[C_\infty Re_{\infty,d}]^{\frac{1}{2}}\int_0^{y/d}\frac{\rho_e u_e}{\rho_\infty u_\infty}\frac{\rho}{\rho_e}\,d(y/d)$ - modified Howarth coordinate

α $\left[1-\frac{4\Delta}{\tilde U^2}\right]^{\frac{1}{2}}$

γ specific heat ratio

δ boundary-layer thickness

δ_b base boundary-layer thickness

δ^* $\int_0^\delta\left(1-\frac{\rho u}{\rho_e u_e}\right)dy$ - boundary-layer displacement thickness

$\Delta(\tilde X)$ $\frac{F(0)''}{\sigma(\tilde X)^2}$ - self-similar profile curvature at $\tilde Y = 0$

* Work supported by A.R.O. and A.R.P.A. under Contract DA-31-124-ARO(D)-33

θ $\int_0^{\delta} \frac{\rho u}{\rho_e u_e}(1 - u/u_e)dy$ - momentum thickness; angle from forward stagnation point

ν kinematic viscosity coefficient

ξ $X - X_N$ - transformed Howarth coordinate

ξ_0 virtual origin for the asymptotic far wake

ρ density

$\sigma(\tilde{X})$, $\sigma(X)$ non-dimensional length scale for the self-similar profiles

ψ stream function

Subscripts

b base stagnation point

$\mathfrak{C}$ centerline

e external

i injected fluid

N neck

s boundary layer immediately upstream of separation

o total or stagnation condition

∞ undisturbed free-stream conditions

Introduction

The roles of heat and mass transfer in the development of the wake behind a body, and the diffusion of chemical species within the near- and far-wake flows are problems of considerable technological importance. The purpose of the present investigation was to determine the effect of mass addition on the laminar wake of a circular cylinder and to examine the diffusion of the injected species within the near-wake flow. The details of this work are given in Reference (1).

The basic flow-field structure for the circular cylinder (Figure (1)), in the absence of mass addition, has previously been described in considerable detail in References (2), (3), (4), (5), and therefore only those aspects of the flow which relate directly to the phenomena of mass addition will be included here. The problem of mass diffusion in the far wake of a uniformly porous cylinder has been discussed in References (6), (7), and Herzog[8] has investigated the effects of nitrogen addition from the base on the near-wake pressure field.

It seems obvious, a priori, that mass addition into the near-wake flow from the base will perturb the flow-field structure. However, it is not obvious what effects on the near wake will be produced by mass addition from the forward stagnation region of the body when the mass transfer rates are low enough that the bow shock structure is not affected. In the latter case, one might expect perturbations to occur in the structure of the cylinder boundary layer which, after separation, becomes the free shear layer in the near wake. For the addition of a foreign species, one might also anticipate changes in the dynamics of the reattaching streamline resulting from the presence of finite mass concentrations. The accumulation of these effects would be expected to influence the near-wake flow field according to the theories of Korst[9] and Chapman.[10][11]

For mass addition from the base, two fundamentally different mechanisms have been proposed to describe the influence of mass addition on the base pressure. These will be briefly summarized:

1. Korst, et. al.[9] proposed for turbulent flow that the base pressure is established by an expansion of the gas from the free-stream direction to a direction parallel to an assumed, straight $\psi=0$ streamline which bounds the recirculating flow, and that the change in base pressure with mass addition can be calculated by considering the spread of the $\psi=0$ streamline to accomodate the added mass.

2. The arguments advanced by Chapman,[10][11] for a fully-developed laminar mixing-layer profile, establish the base pressure in terms of the velocity u* on the stagnating streamline. When the mass entrainment in the shear layer is partially satisfied by mass addition, u* is reduced below the value for a fully-developed free shear layer. As a result, the less energetic compression supports a smaller pressure rise to reattachment, and the base pressure is increased. In the absence of definitive experiments, it has been generally believed that this criterion is correct for laminar flow when modified to include the influence of a finite initial boundary layer on the development of the non-similar mixing profile

The arguments by Korst, et. al., and by Chapman, both conclude that the base pressure, and hence the near-wake structure, depend only on the properly normalized mass flux of the injected fluid. The experiments of Carriére[12] and Ginoux,[13] using only air as an injectant, seem to substantiate the dependence of the base pressure on the mass flux of the injected gas. However, because the distinction between the mass flux and the momentum flux can only be made by varying the molecular weight of the injectant, both sets of experiments are inconclusive. The present experiments are designed to study the physical mechanism associated with the effect of mass addition on the base pressure and the near-wake pressure field, and to determine the correlation of these effects with Reynolds number and molecular weight by using argon, nitrogen and helium as injectants.

To the present time, no theoretical or experimental investigations have been performed to determine the distribution in the near-wake flow field of mass species transferred to the flow from the body. In the present investigation, the distributions of the injected species were measured in the steady near-wake flow of a circular cylinder, and the important mechanisms that determine the distribution of passive scalars (i. e. mass and, by analogy, temperature) in the near wake are examined. In addition, to understand the behavior of the asymptotic far-wake distribution of the injected species, an intermediate wake region, immediately

downstream of the wake neck, is examined to determine the influence of the near-wake flow on the development of the asymptotic far wake.

Experimental Technique

Flow Facility

The experiments were performed at a nominal free-stream Mach number of 6.0, and free-stream Reynolds numbers $Re_{\infty,d} = 0.905 \times 10^4$ and 2.95×10^4 in Leg I of the GALCIT hypersonic facility. This facility is a closed return, continuous flow tunnel with a 5 in. x 5 in. test section and a stagnation temperature of 735° R.

Models

The wind-tunnel models used in this investigation (Figure 1) consisted of 0.200 inch diameter stainless-steel tubes which spanned the test section and were supported by dual O-ring seals in ports on either side wall. These models were provided with triangular cross-flow fences downstream of the cylinder to insure a spanwise uniform static-pressure field in the base region (cf. Reference (1)).

Two models were used in the experiments: a pressure model and a mass transfer model. The pressure model used an internal O-ring to hold either base mounted Pitot probes or insert static-pressure probes, with which the axial distributions of Pitot and static pressure were measured in the reversed flow in the absence of mass addition. The mass transfer model (Figure 1) used a machineable porous ceramic insert, bonded with epoxy into a longitudinal slot in the cylinder, to transfer the injectant from the body surface into the flow field at a rate determined by a calibrated flow meter. Pressure taps were not included in the model because of the small scale and the possibility of interference with the flow through the ceramic material.

To insure the spanwise uniformity of the flow field, the model plenum pressure and temperature were measured. The pressure was found to be uniform with 0.5% and independent of the external flow, while the temperature was within 10% of the adiabatic-wall temperature of the model. It is concluded that the flow through the ceramic is an isothermal, choked flow and that the exit Mach number $M_i \sim 1/\sqrt{\gamma_i}$. Measurements of the spanwise pressure and mass-concentration distributions in the base region confirmed that the near-wake flow with mass addition was nearly two-dimensional in the region of reversed flow. Downstream of reattachment, three-dimensional effects resulted in an overall decrease in the mass-concentration levels.

Pressure Measurement

The impact-pressure and mass-concentration fields were measured by using a family of Pitot-sampling probes, constructed with various dimensions for the flattened oval tip, in order to investigate the effects of probe Reynolds number and to provide an adequate sample with a minimum probe dimension and minimum response time. The static-pressure field was also measured using a family of probes, each adapted to the particular regime of measurement (cf. Reference (1)).

The measurements were made with a 0-5 psia pressure transducer manufactured by Statham Instrument Co., and a vacuum reference silicone-oil micromanometer. The data were corrected for both viscous and probe interference effects, and were adjusted to account for existing tunnel gradients.

Mass Concentration Measurement

Reis and Fenn[14] have demonstrated that for the flow of a binary mixture of gases of disparate molecular weights, the presence of a sampling probe may cause barotropic species separation by virtue of the existence of a strong lateral pressure gradient in the vicinity of the probe tip. The magnitude of this separation is a function of the Mach number, Reynolds number, and the disparity between the constituent molecular weights. The important parameter in the mass-sampling problem is the ratio of the area of the sampled stream tube relative to the incident cross-section of the probe, which, for the low Reynolds numbers encountered in the present experiments, is typically of the order of 0.2, because of viscous effects.

To verify that the mass concentrations measured by the probe were correct, measurements were performed in the wake behind the cylinder, with mass addition from the base. For these measurements, the mass concentration at a point was measured as a function of probe Reynolds number and the mass flux through the probe, for argon and helium addition. No barotropic effects were found either for an increase in probe Reynolds number by a factor of five, or for a change in probe mass flux by a factor of ten. On the basis of these measurements, it is concluded that the sample obtained is representative of the undisturbed flow field.

The detector for the mass-analysis system was a Varian Associates Partial Pressure Gauge, a small magnetic mass spectrometer utilizing a modified Bayard-Alpert source with a thoriated-iridium filament. The spectrometer background pressure was maintained at 2×10^{-8} torr by a liquid-nitrogen-trapped oil diffusion pump. During operation, a continuous sample was throttled to a known, constant pressure (25μ) maintained by a trapped mechanical pump, and a portion of the sample was expanded through a fixed capillary into the spectrometer, operating at a pressure of 2×10^{-6} torr.

The spectrometer system was calibrated using known mixtures. A single peak was scanned for each binary mixture, i.e. m/e = 40 for argon-air and m/e = 28 for both nitrogen-air and helium-air, and the output of the spectrometer was recorded, normalized by the spectrometer output for the pure gas under the same inlet conditions.

For argon, the error in the measurements was at most 1.5% of the measured value over the entire range of mass concentrations. For a 1% error in the measurement of nitrogen, however, the percent error in the mass concentration of the added nitrogen becomes unbounded as zero concentration is approached, because the background gas (air) contains ~80% nitrogen. The helium mass concentrations

were also measured using the m/e = 28 peak of nitrogen because of an instability which occurred in the m/e = 4 peak of helium. Therefore the error for helium also becomes unbounded for vanishing mass concentrations. However, as in the case of nitrogen, the percentage error rapidly dimishes with increasing mass concentration of helium.

The Structure of the Flow Field with Mass Addition

Forward Injection

Measurements of the near-wake pressure field for mass addition from the forward stagnation region demonstrate that the Pitot-pressure distributions and the base pressure (Figure 2) are completely independent of mass addition although the mass transfer rates are large compared to the local boundary-layer mass flux in the vicinity of the stagnation point. The measurements show that neither the bow shock wave nor the Pitot-pressure distributions in the boundary layer upstream of separation are altered by moderate mass addition rates. The dynamics of the flow along the dividing streamline are unaltered because the near-wake mass concentrations are sufficiently low that the density and specific heats ratio γ are essentially constant.

On the basis of these measurements, it is concluded that the mass-concentration field corresponding to moderate rates of mass addition from the forward stagnation region is simply the field of a scalar quantity diffusing from an initial distribution in the cylinder boundary layer into the otherwise undisturbed near-wake flow.

Mass Addition from the Base

Base Pressure

The most important result of the present experiments is that neither the Korst nor the Chapman theory outlined in the Introduction gives a proper description of the behavior of the base pressure with base mass transfer. The present experiments show that, under the condition that a non-vanishing recirculating flow exists in the near wake, the base pressure (Figure 2), and the entire near-wake pressure field (Figure 5) correlate with the injection parameter

$$I = \frac{\dot{m}_i}{2\dot{m}_{B.L.}}\sqrt{\frac{\mathcal{M}_{Air}}{\mathcal{M}_i}}$$

This parameter is the momentum flux of the injected fluid, properly normalized to account for the influence of free-stream Reynolds number and the molecular weight of the injectant.

The present experiments suggest a physical model for the base pressure which depends on the dynamics of the interaction of the injected gas with the recirculating near-wake flow field. This model possesses two aspects: (1) the interaction of the injected fluid with the reversed flow forms a stagnation point off of the body, and consequently (2) the injected fluid is turned away from the axis and is impressed on the free shear layer near its origin, inducing an increase in pressure. Both aspects are coupled and result in a momentum flux dependence for the base pressure.

The primary aspect of this model is the interaction between the injected fluid and the reversed flow. For moderate mass addition rates, a recirculating vortex remains in the near wake, and hence two stagnation points exist on the axial streamline: the rear stagnation point, and a stagnation point in the vicinity of the base (see Figure 1). Figure (3) demonstrates that the total pressure of the injected gas is comparable with the total pressure on the centerline of the recirculating vortex, and hence the base stagnation point is formed off the body by a balance between the total pressures of the two interacting streams. The generalization of the base pressure, or characteristic near-wake pressure, is the stagnation pressure of the highly dissipative reversed flow at the base stagnation point,* and is therefore determined by the momentum flux of the injected fluid. The proper scaling for this momentum flux is given by the momentum flux of the reversed flow.

The total pressure on the axial streamline decays monotonically from its value at the rear stagnation point to its value at the base stagnation point as a consequence of viscous dissipation. Therefore, as the momentum flux of the injected gas, and hence its total pressure, is increased, the base stagnation point moves toward the rear stagnation point into a region of increasing total pressure for the reversed flow. Simultaneously, the reversed flow is reduced as a consequence of the reduction of the value of u* on the stagnating streamline. For these reasons, the base pressure increases with increasing mass addition. When the total pressure of the injected fluid exceeds the maximum available total pressure in the reversed flow, the entrainment required by the shear layers is satisfied by the injected gas and the reversed flow vanishes, as reported by Herzog.[8]

The second aspect of the model involves the interaction between the injected gas and the separating free shear layer. The gas injected from the base is turned by the reversed flow in a distance $\delta_b = \delta_b(\dot{m}_i/\sqrt{\mathcal{M}_i})$, the distance from the body to the base stagnation point, and is impressed on the separating free shear layer over a distance L, which is of the order of δ_b. The effects on the free shear layer caused by the impressed mass are determined by the amount of mass that the layer is required to entrain. The idealization proposed by Chapman[16] gives an upper bound on the mass entrainment resulting from viscous stresses. If the entrainment is greater than Chapman's value, viscous stresses are no longer sufficient to turn the flow and a pressure increase is induced by the interaction which turns both the impressed flow and the flow in the free shear layer. The amount of the turning of the shear layer flow, and hence the induced pressure, is determined from a balance between the momentum flux of the impressed flow and some characteristic momentum flux associated with the free shear layer.

For the present experiments, the entrainment rate of the impressed fluid,

* This distinction has not been made in the work of Fuller and Reid,[15] for example, and care must be used in the interpretation of their results.

$$-\zeta_0 = \lambda_e \sqrt{\frac{Re_x}{C_\infty}}$$

where $$\lambda_e = \frac{\rho_{-\infty} v_{-\infty}}{\rho_e u_e}$$

exceeds the Chapman value by a factor of from four to eight. Therefore, so long as the entrainment is large compared to the entrainment specified by the Chapman solution, and so long as a recirculating vortex exists in the near wake, the change in the near-wake pressure field with base mass addition will be a function only of the properly normalized momentum flux of the injected gas.

Mass Transfer Parameter

The base stagnation point interaction has determined that the proper scaling for the momentum flux of the injectant is given by the momentum flux in the reversed flow. However, for the circular cylinder, because the sub-critical separation process allows a smooth transition from the cylinder boundary layer to the non-similar laminar free shear layer, the Reynolds number scaling is the same for both the reversed flow and the cylinder boundary layer. Therefore, the characteristic near-wake momentum flux has been taken as that associated with the cylinder boundary layer upstream of separation.

Using these ideas, an injection parameter is formulated from the ratio of the momentum flux of the injected gas to the momentum flux in the boundary layer upstream of separation, given by

$$\Pi = \frac{\dot{m}_i u_i}{2(\rho_e u_e^2)_s \int_0^\delta \left(\frac{\rho u^2}{\rho_e u_e^2}\right)_s dy}$$

Evaluating the integral,

$$\Pi = \frac{\dot{m}_i}{2\dot{m}_{B.L.}} \left[\frac{\mathcal{M}_{Air}}{\mathcal{M}_i}\right]^{\frac{1}{2}} \left\{\frac{M_i}{M_e}\left[\frac{\delta-\delta^*}{\delta-\delta^*-\theta}\right]\left[\frac{T_i}{T_e}\frac{\gamma_i}{\gamma_e}\right]^{\frac{1}{2}}\right\}_s .$$

Since the porous ceramic is isothermally choked, and $T_i \approx T_{aw}$, where T_{aw} is the recovery temperature of the model, therefore, $\Pi = I[F(m_e, \gamma_e)]$, where

$$I = \frac{\dot{m}}{2\dot{m}_{B.L.}} \left[\frac{\mathcal{M}_{Air}}{\mathcal{M}_i}\right]^{\frac{1}{2}}$$

and, for large Reynolds numbers and hypersonic Mach numbers,

$$F(M_e, \gamma_e) = \left\{\frac{1}{M_e\sqrt{\gamma_e}}\left[\frac{\delta-\delta^*}{\delta-\delta^*-\theta}\right]\left[\frac{T_{0_i}}{T_0}\frac{T_0}{T_e}\right]^{\frac{1}{2}}\right\}_s$$

is dependent on $Re_{\infty, d}$ only through the weak dependence of the location of the separation point on $Re_{\infty, d}$, and is assumed to be invariant. The boundary-layer mass flux per unit span upstream of separation was calculated from a locally similar solution given by Klineberg.[3]

Two fundamental differences exist between the present mass transfer criterion and those derived from the models proposed by Korst, et. al.[9] and by Chapman:[10]

1. The present parameter,

$$I = \frac{\dot{m}}{2\dot{m}_{B.L.}} \left[\frac{\mathcal{M}_{Air}}{\mathcal{M}_i}\right]^{\frac{1}{2}}$$

is based on the momentum flux of the injected fluid, not the mass flux as proposed by Korst, for example. It should be noted, however, that when either air or nitrogen are used as the injectant, the parameter I is indistinguishable from a mass flux parameter.

2. The present model assumes that the proper normalization is the momentum flux in the boundary layer upstream of separation, while the Korst parameter,

$$H = \frac{\dot{m}_i}{\dot{m}_f} G(M_\infty)$$

for example, assumes that the proper mass flux normalization is the free-stream mass flux, $\dot{m}_f$. These models differ in the Reynolds number scaling for the mass transfer parameter, as

$$I \sim [Re_{\infty, d}]^{-\frac{1}{2}}$$

whereas $$H \sim [Re_{\infty, d}]^{-1}$$

Figure (2) clearly demonstrates that both the Reynolds number and molecular weight scaling are properly included in the momentum criterion for the mass transfer regime considered.

In view of the present results, it is clear that the role of momentum can only be determined by an investigation of the effect of molecular weight. For this reason, the results reported by Carriére[12] and by Ginoux,[13] for example, appear to be inconclusive.

Pressure Field Similitude

The transverse Pitot-pressure profiles at the neck, shown in Figure (4) for nitrogen addition at $Re_{\infty, d} = 3\times10^4$, illustrate the major features of the influence of increasing mass addition on the near-wake flow field. With increasing mass addition, the location of the separation point moves forward on the cylinder (cf. Herzog[8]), and the separation shock is displaced into the outer, rotational flow with a corresponding increase in strength. In addition, the spreading of the viscous layers results in a pronounced decrease in the strength of the wake, or recompression shock, and the combined effects significantly influence the development of the intermediate- and far-wake flows, downstream of the wake neck.

The correlation of the Pitot-pressure field with the mass addition parameter for argon, nitrogen and helium addition is shown in Figure (5) for a single value of $Re_{\infty, d}$ at two selected axial locations; x/d = 0.75 lies within the recirculating vortex, and x/d = 3.0 is the location of the wake neck also shown in Figure (4). The correlation of the entire pressure field, for both values of $Re_{\infty, d}$, has not been included here. This correlation is demonstrated in Reference (1) where, in addition, the separation and wake shock wave locations are

shown as a function of increasing I to conclusively demonstrate the complete pressure field correlation.

The Structure of the Mass-Concentration Field

The Near-Wake Flow

Mass Addition From the Base

The results for the near-wake mass-concentration field with mass addition from the base are given in Figures (6), (7) and (8). Figure (6) is an isometric plot of the argon mass-concentration field, while Figures (7) and (8) are isograms of the argon and helium mass-concentration fields respectively, overlayed on the characteristic features of the corresponding pressure field. In each of these figures the mass-concentration field is displayed for the same value of I and for each of the two values of Reynolds number.

Figures (6) and (9) demonstrate that the dominant feature of the near-wake mass-concentration field is the axial decay of the mass concentrations from the base toward the rear stagnation point as a result of the counter-current diffusion of the injected species into the reversed flow. A second important aspect of the mass-concentration field is the existence of an outer transport layer, shown in Figure (6). This outer layer occurs in the vicinity of the shear layers and governs the transport of mass between the recirculating vortex and the outer flow of diffusion across the shear layers, thus establishing the outer boundary condition on the inner recirculating flow.

For $Re_{\infty, d} = 3 \times 10^4$, the transverse mass-concentration profiles illustrated in Figure (6) are characterized by an off-axis maximum in the vicinity of the u = 0 locus as a result of the convection of the high mass-concentration layer near the base into the shear layer by the recirculating flow. This maximum appears as a folding of the isolines in Figure (7) and isolates the outer transport layer from the mass-concentration field near the axis. Lateral and axial diffusion result both in the decay of this maximum, as the rear stagnation point is approached, and the subsequent development of the profile toward the asymptotic Gaussian form downstream of the rear stagnation point. For $Re_{\infty, d} = 0.9 \times 10^4$, the mass-concentration field is diffusion dominated within the recirculating zone. At this lower Reynolds number, the local maximum does not exist and the outer transport layer is no longer distinct (Figures (6),(7)). The decreased Schmidt number for helium (Figure (8)) results similarly in the increased role of diffusion, a consequent reduction of the off-axis maximum for $Re_{\infty, d} = 3 \times 10^4$, and a more rapid transformation to a monotonic diffusion profile.

From this brief description of the mass-concentration field, a close analogy can be seen between the present experiments and the theoretical model proposed by Scott and Eckert[17] for heat transfer in high Reynolds number separated flows. Scott and Eckert have postulated the existence of two thin layers to describe the transport of heat between the body and the outer flow. The first layer in their model, a boundary layer at the base, governs the transport of heat or mass at the body surface. In the following discussion, the axial profile given in Figure (9) will be shown to correspond to a generalization of the concept of a base boundary layer for the low Reynolds numbers encountered in the present experiments. The second layer in the model proposed by Scott and Eckert corresponds closely with the outer transport layer observed in the experiments, and governs the transport of heat or mass between the recirculating vortex and the outer flow. Again, this outer layer may not be thin, as a consequence of the low Reynolds numbers encountered in the experiments.

The boundary conditions on the mass-concentration distribution in the recirculating flow are determined by the mass concentration at the base and by the diffusional loss of mass through the outer transport layer. The mass-concentration distribution along the u = 0 locus, and hence the mass concentration at the rear stagnation point, is determined from the requirement that the net efflux from the recirculating region exactly balances the mass added.

To obtain a qualitative description of the axial distribution of mass concentration in the region between the two stagnation points, an approximate solution of the species conservation equation on the axis will be obtained subject to the boundary conditions on the mass concentration at the base and at the rear stagnation point. From Figure (6), it is apparent that both the axial and the transverse diffusion terms in the species conservation equation must be retained on the axis. If ρD = const., and both thermal and barotropic diffusion are ignored, then for

$$\tilde{X} = \frac{x - x_b}{x_r - x_b} \quad , \qquad \tilde{Y} = \frac{y}{x_r - x_b}$$

where x_b is the location of the base stagnation point in physical coordinates, the species equation takes the non-dimensional form

$$\frac{\partial^2 C_i}{\partial \tilde{X}^2} + \frac{\partial^2 C_i}{\partial \tilde{Y}^2} + \tilde{U}(\tilde{X}) \frac{\partial C_i}{\partial \tilde{X}} = 0 \ ,$$

where $\tilde{U}(\tilde{X}) = \frac{u(\tilde{X})}{u_{max}} \cdot \frac{|u_{max}|(x_r - x_b)}{D} = Re(\tilde{X})Sc$.

To facilitate a solution, the mass-concentration field near the axis is assumed to be self-similar, i.e. $C_i = C_{\mathbb{C}}(\tilde{X})\ F(\tilde{Y}/\sigma(\tilde{X}))$.

Then $\left.\frac{\partial^2 C_i}{\partial \tilde{Y}^2}\right|_{\tilde{Y}=0} = C_{\mathbb{C}}(\tilde{X}) \frac{F_{(o)}''}{\sigma(\tilde{X})^2} = \Delta(\tilde{X})\, C_{\mathbb{C}}(\tilde{X})$,

and the axial species conservation equation becomes

$$\frac{d^2 C_{\mathbb{C}}}{d\tilde{X}^2} + \tilde{U}(\tilde{X}) \frac{dC_{\mathbb{C}}}{d\tilde{X}} + \Delta(\tilde{X})\, C_{\mathbb{C}}(\tilde{X}) = 0 \ .$$

For a qualitative understanding of the concentration field, it is sufficient to make the assumption that $\tilde{U}(\tilde{X})$ and $\Delta(\tilde{X})$ are independent of $\tilde{X}$. Then the species equation has the solution

$$C_{\mathbb{C}}(\tilde{X}) = A\, e^{\frac{\tilde{U}}{2}(\alpha - 1)\tilde{X}} + B\, e^{-\frac{\tilde{U}}{2}(\alpha + 1)\tilde{X}}$$

where $\alpha = \left[1 - \frac{4\Delta}{\tilde{U}^2}\right]^{\frac{1}{2}}$

Taking the boundary conditions at $\tilde{X} = 0, 1$, the constants become

$$A = -\frac{\left[C_{\tilde{\xi}}(0)\, e^{-\tilde{U}\alpha} - C_{\tilde{\xi}}(1)\, e^{-\frac{\tilde{U}}{2}(\alpha-1)}\right]}{\left[1 - e^{-\tilde{U}\alpha}\right]}$$

$$B = \frac{\left[C_{\tilde{\xi}}(0) - C_{\tilde{\xi}}(1)\, e^{-\frac{\tilde{U}}{2}(\alpha-1)}\right]}{\left[1 - e^{-\tilde{U}\alpha}\right]}$$

It is apparent from these results that the presence of the rear stagnation point imposes as the solution to the species equation the linear superposition of a positive and a negative exponential function. The negative exponential corresponds to the decay from a source at the base stagnation point into a uniform flow of infinite extent with lateral diffusion; whereas, the positive exponential represents the decay toward the base of the mass concentration supplied by a source at the rear stagnation point, whose strength is determined by the outer flow.

As $\tilde{U} = ReSc \to \infty$, the boundary-layer character of the solution becomes evident. In this limit $\alpha \approx 1$, and the solution becomes

$$C_{\tilde{\xi}}(\tilde{X}) = C_{\tilde{\xi}}(0)\, \frac{\left[e^{-\tilde{U}\tilde{X}} - e^{-\tilde{U}}\right]}{\left[1 - e^{-\tilde{U}}\right]} + C_{\tilde{\xi}}(1)\, \frac{\left[1 - e^{-\tilde{U}\tilde{X}}\right]}{\left[1 - e^{-\tilde{U}}\right]}$$

Thus, for large Reynolds numbers, the injected species is confined to a thin, exponentially decaying boundary layer with a characteristic thickness $\delta_b \sim \tilde{U}^{-1}$. This solution corresponds to the thin base boundary layer proposed by Scott and Eckert. (17)

In the present experiments, $\tilde{U} = ReSc \sim 0(1)$, and the axial diffusion depth is of the order of the distance between the two stagnation points, $\delta_b \sim \tilde{U}^{-1} \approx 1$. Under these circumstances, the near-wake axial distribution given in Figures (6) and (9) represents a generalization to low values of $\tilde{U} = ReSc$ of the concept of a thin base boundary layer proposed by Scott and Eckert. The two length scales in the solution, $\tilde{X} \sim \tilde{U}^{-1}$ and $\tilde{X} \sim (\Delta)^{-\frac{1}{2}} \sim \sigma/(|F_o''|)^{\frac{1}{2}}$ are derived from the influence of counter-current diffusion and of transverse diffusion, respectively.

Forward Injection

For argon addition from the forward stagnation region, the near-wake mass-concentration field is illustrated in the isometric plot in Figure (10) and the isogram in Figure (11). In both figures, the same value of the mass transfer parameter $\dot{M} = (\dot{m}_i)/(2\dot{m}_{B.L.})$ is used at each of the two values of Reynolds number.

The species transferred from the forward stagnation region enter the near-wake flow field through mass-concentration boundary layers whose thickness upstream of separation is comparable to the viscous boundary-layer thickness. The mass concentration distribution in these boundary layers dominates the boundary conditions for the distribution of mass concentration in the near-wake flow field, and sets the mass-concentration level at the base. The extensions of the boundary layers into the near-wake flow are the narrow mass-transport layers shown in Figure (10). These layers form the outer transport layers in the two layer model proposed by Scott and Eckert, (17) and thus provide the outer boundary conditions on the mass-concentration field in the region of reversed flow.

The transverse mass-concentration profiles for argon exhibit a nearly uniform region between the $u = 0$ loci (Figure(11)) as a consequence of the effects of transverse diffusion within the recirculating vortex and of the decrease in the mass concentration along the undisturbed dividing streamlines by the diffusional loss of the injected species through the outer transport layers. This latter fact results in a reduction of the mass concentration level at the rear stagnation point below that at the base and provides the second boundary condition for the axial decay of mass concentration in the near wake. A local maximum occurs off the axis, followed by a rapid decay of the mass concentration in the outer transport layer. The local maximum also occurs in the boundary-layer profiles in the immediate vicinity of separation, but does not persist further upstream.

The near-wake mass-concentration profiles for helium exhibit the dominant role of diffusion. For $Re_{\infty, d} = 3 \times 10^4$, a local maximum again occurs near the base, but decays rapidly downstream because of the decreased Schmidt number. For $Re_{\infty, d} = 0.9 \times 10^4$, the profiles exhibit a single inflection point similar to the profiles shown in Figure (6) for argon addition from the base at the same Reynolds number. The details are given in Reference (1).

To obtain a qualitative understanding of the mass-concentration field in the present case, the approximate solution given previously for the axial distribution can again be used. For the present case, because the transverse distribution is nearly uniform, $\Delta = 0$ and hence $\alpha = 1$. Therefore the solution of the axial species conservation equation,

$$C_{\tilde{\xi}}(\tilde{X}) = C_{\tilde{\xi}}(0)\, \frac{\left[e^{-\tilde{U}\tilde{X}} - e^{-\tilde{U}}\right]}{\left[1 - e^{-\tilde{U}}\right]} + C_{\tilde{\xi}}(1)\, \frac{\left[1 - e^{-\tilde{U}\tilde{X}}\right]}{\left[1 - e^{-\tilde{U}}\right]},$$

has the same form as obtained for $\tilde{U} \to \infty$ in the previous discussion. However, in the present case, $\tilde{U} = ReSc \sim 0(1)$ as before, and hence $\delta_b \sim \tilde{U}^{-1} \approx 1$, i.e. the axial diffusion depth is of the order of the distance between the two stagnation points. Furthermore, because there is no source in the base region, the difference between the mass-concentrations at the base and at the rear stagnation point results only from the decrease in the mass concentration of the injected species along the dividing streamline by diffusional loss through the outer transport layer. As a result, the two boundary conditions are nearly equal and the axial decay is extremely weak compared to that for base mass addition (cf. Figures (6), (9) and (10)). As $\tilde{U} \to \infty$, the exponential functions again represent a thin boundary layer at the

base. However, because no source exists at the base, the mass-concentration field is not expected to exhibit a boundary layer behavior. On the contrary, as $\bar{U}$ becomes large, convection will dominate over diffusion and it is expected that the mass concentration of the injectant will be uniformly distributed within the recirculating flow, i. e. $C_{\mathfrak{L}}(1) \rightarrow C_{\mathfrak{L}}(0)$.

The Intermediate Wake

When the Oseen linearization used by Kubota[18] to determine the asymptotic self-similar form for the inner wake is extended to the mass-concentration wake, the asymptotic far-wake solution corresponds to the diffusion from a delta function source at the origin,

$$C_i = \frac{\dot{m}_i}{2\rho_\infty u_\infty d}\left[\frac{C_\infty Re_{\infty,d}\, Sc}{\pi}\right]^{\frac{1}{2}} \frac{e^{-\frac{Sc\,Y^2}{4X}}}{\sqrt{X}}$$

where the details of the near-wake may be lumped in the description of a virtual origin of the axial coordinate.

As a transition from the near wake to the asymptotic far wake, the presence of the rear stagnation point, and the finite width of the mass-concentration profiles at the neck, require that there also be an intermediate-wake region in which the mass-concentration and velocity fields experience a transition from those distributions imposed at the rear stagnation point by the near-wake flow to their respective asymptotic far-wake distributions. The boundary conditions for the intermediate wake solution are specified by the mass-concentration distribution at the neck. In the incompressible plane, Figure (12) shows that for argon the measured transverse mass-concentration profiles in the vicinity of the neck rapidly approach a Gaussian form with increasing axial distance. These profiles exhibit a characteristic width $Y = \sigma(X)$, for which $C_i/C_{\mathfrak{L}} = 1/e$, and their amplitudes $C_{\mathfrak{L}}$ scale linearly with increasing mass transfer. In addition, the experiments indicate that the lateral scale for the mass-concentration wake depends mechanically on the lateral scale for the viscous wake, independent of the mass transfer rate.

Using these experimental observations, an approximate solution for the axial distribution of argon mass concentrations will be obtained for $Re_{\infty,d} = 0.9\times10^4$. This result is not extended to the data for $Re_{\infty,d} = 3\times10^4$ because of the occurrence of transition in the intermediate-wake flow field at this Reynolds number. The case of helium addition will be mentioned separately.

Neglecting axial diffusion, the species conservation equation on the axis becomes

$$u/D\,\frac{\partial C}{\partial x} = \frac{\partial^2 C}{\partial y^2}$$

In addition, conservation of the injected species provides the integral relation

$$m_i = 2\int_0^\infty \rho u\, C_i\, dy = \text{const.}$$

Using the modified Howarth transformations to the incompressible plane, these equations take the form

$$Sc\; U\,\frac{\partial C}{\partial X} = \frac{\partial^2 C}{\partial Y^2}$$

$$\int_0^\infty UC\,dY = \int_0^\infty UC\,dY \quad ,$$

$$N \qquad\qquad X$$

where $Sc = \nu/D = \text{const.}$

To simplify the calculations, it is convenient to assume that both the mass-concentration and the velocity fields have Gaussian distributions, and possess the same scale, i. e.

$$\frac{C}{C_{\mathfrak{L}}(X)} = \frac{1-U}{1-U_{\mathfrak{L}}(X)} = e^{-Y^2/\sigma^2(X)} \quad .$$

Under these conditions, the equations reduce to

$$Sc\; U_{\mathfrak{L}}(X)\frac{dC_{\mathfrak{L}}(X)}{dX} = -\frac{2C_{\mathfrak{L}}(X)}{\sigma(X)^2}$$

$$\sigma(X) = \frac{\sigma_N C_N [b+U_N]}{C_{\mathfrak{L}}(X)\,[b+U_{\mathfrak{L}}(X)]}$$

where $b = \sqrt{2} - 1$ for a Gaussian profile. Combining these relations, the species equation becomes

$$\frac{[b+U_{\mathfrak{L}}(X)]^2}{U_{\mathfrak{L}}(X)}\,dX = -\frac{Sc\,\sigma_N^2 C_N^2}{2}[b+U_N]^2\,\frac{dC_{\mathfrak{L}}(X)}{C_{\mathfrak{L}}(X)^3}$$

To approximate the axial velocity distribution, an analytic form which has the proper limiting behavior for small X,

$$U_{\mathfrak{L}} = \frac{X}{a+X}$$

has been obtained by matching the experimental data at X = 4.0. Using this relation, if the origin and the boundary conditions are taken at the neck, the solution becomes

$$\frac{C_{\mathfrak{L}}(\xi)}{C_N} = \left\{1 + \frac{8}{Sc\,\sigma_N^2[b+U_N]^2}\left[\xi - \frac{a}{2}\ln\left(\frac{a+X_n+\xi}{a+X_N}\right) + \left(\frac{3}{2}-\sqrt{2}\right)a\ln\left(\frac{X_N+\xi}{X_N}\right)\right]\right\}^{-\frac{1}{2}} ,$$

where $\xi = X - X_N$. For small ξ, $\frac{C_{\mathfrak{L}}(\xi)}{C_N} \rightarrow 1-\beta\xi$

For large ξ, $\frac{C_{\mathfrak{L}}}{C_N} \rightarrow (\beta^*\xi)^{-\frac{1}{2}}$, where

$$\beta^* = \frac{8}{Sc\,\sigma_N^2[b+U_N]^2}$$

Thus, for large ξ the solution approaches the decay law given by the Oseen linearized solution.

The virtual origin is then given as $\xi_o = 1/\beta^* \sim Sc\sigma_N^2$, and is shown by the extrapolation of the solution curve in Figure (13).

The normalized solution contains a single parameter σ_N, the scale of the transverse profile at the neck. This parameter depends on the distribution in the near-wake flow field, and has been obtained from experiment by matching the data at an arbitrary value of ξ. The results are shown in Figure (13) for argon addition from both the forward and the base stagnation regions.

For helium addition, the near-field solution for $\xi \to 0$ is invalid because the axial diffusion term is not negligible near the origin. The far-field solution is valid, however, and has been used in Reference (1) to further substantiate dependence of the virtual origin on $Sc\sigma_N^2$ for the asymptotic far wake.

Summary

An experimental investigation of the steady, laminar near-wake flow field of a two-dimensional, adiabatic, circular cylinder with surface mass transfer has been made at a free-stream Mach number of 6.0, and free-stream Reynolds numbers $Re_{\infty, d} = 0.9$ and 3.0×10^4.

The purpose of the investigation was to determine the effects on the near-wake flow field associated with the addition of mass from the body surface. The pressure and mass-concentration fields associated with the transfer of argon, nitrogen or helium into the near-wake were studied for mass transfer from the forward stagnation region and for mass transfer from the base.

Mass addition from the forward stagnation region has no measurable influence on the near-wake pressure field for moderate mass transfer rates.

For mass addition from the base, the present experiments conclusively demonstrate that the base pressure, and the entire near-wake flow field, correlates with the parameter

$$I = \frac{\dot{m}_i}{2\dot{m}_{B.L.}}\sqrt{\frac{m_{Air}}{m_i}} = \frac{\text{const. } \dot{m}_i}{\sqrt{Re_{\infty, d}}}\sqrt{\frac{m_{Air}}{m_i}}$$

the ratio of the momentum flux of the injected fluid to the momentum flux in the cylinder boundary layer upstream of separation. The mechanism which determines the behavior of the base pressure with mass addition is the establishment of a stagnation point off the base, formed by the balance of momentum between the injected fluid and the reversed flow, and the consequent impression of the injected gas on the free shear layer near separation.

The distinction between a mass flux and a momentum flux parameter is only possible through the use of injectants with molecular weights different from that of the free stream. When the molecular weight of the injectant is equal to that of the free stream, the parameter I is indistinguishable from a mass flux parameter. For this reason, previous investigations (References (12), (13)), using only air as an injectant, cannot be used to demonstrate the dependence of the base pressure on the mass flux of the injectant. Indeed, whether any such regime exists in which the near-wake flow field correlates with the mass flux of the injectant is not clear. Such a regime does not exist in the present measurements even for vanishingly small changes in base pressure.

For large values of mass addition, for which the mass entrainment in the shear layers is satisfied by the injection, no recirculating flow exists. For this regime, the measurements of Lewis and Behrens[19] have demonstrated that the changes in the pressure field depend on the volume flow of the injectant. This regime has not been investigated in the present experiments.

The mass-concentration distribution in the near wake depends entirely on the boundary conditions on the body and on the product ReSc.

For mass addition from the base, the base mass concentration is large, and the dominant feature of the mass-concentration field is the rapid axial decay away from the base as a consequence of the counter-current diffusion of the injected species into the reversed flow. The transverse profiles decay rapidly away from the centerline and, at the higher Reynolds number, possess a local minimum in the vicinity of the $u = 0$ locus as a consequence of the convection of the high mass-concentration layer near the base into the outer flow by the recirculating vortex. The recirculating flow is bounded by outer transport layers in the vicinity of the shear layers which dominate the transport of mass into the outer flow.

For mass addition from the forward stagnation region, the injected mass enters the near wake through the boundary layers on the cylinder. Because no source exists at the base, the mass-concentration field is nearly uniform in the region of reversed flow, and possesses a local maximum in the vicinity of the $\psi = 0$ streamline. The weak axial decay observed in the experiments results only from the decrease in the mass concentration of the injected species along the dividing streamline by diffusional loss through the outer transport layers.

In the intermediate-wake region, downstream of the neck, the mass-concentration field has been examined with the aid of an approximate theoretical model which assumes that the mass-concentration distribution is Gaussian in the incompressible plane. For argon addition, the axial diffusion terms are negligible and the species conservation equation on the axis gives a representation for the axial decay. By comparison with the experimental data, the solution yields the axial distribution, and the location of the virtual origin for the asymptotic far-wake solution, as a function of the distribution of mass concentration at the wake neck. The analysis for helium requires that the axial diffusion term be retained, and has not been presented here.

References

1. Collins, D. J.: "The Near Wake of a Two-Dimensional Hypersonic Blunt Body with Mass Addition," Ph. D. Thesis, California Institute of Technology, Pasadena, California (Dec., 1968).

2. Reeves, B. L. and Lees, L.: "Theory of Laminar Near Wake of Blunt Bodies in Hypersonic Flow," AIAA J., 3, No. 11, 2061 (Nov., 1965).

3. Klineberg, J. M.: "Theory of Laminar Viscous-Inviscid Interactions in Supersonic Flow," Ph. D. Thesis, California Institute of Technology, Pasadena, Calif. (1968).

4. McCarthy, J. F., Jr.: "Hypersonic Wakes," GALCIT Hypersonic Research Project, Memorandum No. 67 (July, 1962).

5. Behrens, W.: "The Far Wake behind Cylinders at Hypersonic Speeds. Part I: Flowfield," AIAA J., 5, No. 12, 2135 (Dec., 1967). "Part II. Stability," AIAA J., 6, No. 2, 225 (February, 1968).

6. Mohlenhoff, W.: "Experimental Study of Helium Diffusion in the Wake of a Circular Cylinder at M = 5.8," GALCIT Hypersonic Research Project, Memorandum No. 54 (May, 1960).

7. Kingsland, L.: "Experimental Study of Helium and Argon Diffusion in the Wake of a Circular Cylinder at M = 5.8," GALCIT Hypersonic Research Project, Memorandum No. 60 (June, 1961).

8. Herzog, R. T.: "Nitrogen Injection into the Base Region of a Hypersonic Body," GALCIT Hypersonic Research Project, Memorandum No. 71 (August, 1964).

9. Korst, H. H., Page, R. H. and Childs, M. E.: "A Theory for Base Pressures in Transonic and Supersonic Flow," University of Illinois, Engineering Experiment Station, M. E. Technical Note - 392-2 (March, 1955).

10. Chapman, D. R.: "Theoretical Analysis of Heat Transfer in Separated Flows," NACA TN-3792 (1956).

11. Chapman, D. R., Kuehn, D. M. and Larson, H. K.: "Investigation of Separated Flows in Supersonic and Subsonic Streams with Emphasis on the Effects of Transition," NACA TN-1356 (1958).

12. Carriére, P.: "Recherches Récentes Effectuées A L'O. N. E. R. A. Sur les Problémes de Recollement," O. N. E. R. A. T. P. No. 275 (1965).

13. Ginoux, J. J.: "Effects of Gas Injection in Separated Supersonic Flows," TCEA TN-7 Von Kármán Institute, Rhode-Saint-Genese, Belgium (February, 1962).

14. Reis, V. H. and Fenn, J. B.: "Separation of Gas Mixtures in Supersonic Jets," J. Chem. Phys., 39, No. 12, 3240 (Dec., 1963).

15. Fuller, L. and Reid, J.: "Experiments on Two-Dimensional Base Flow at M = 2.4," A. R. C. -R & M #3064 (British), (1958).

16. Chapman, D. R.: "Laminar Mixing of a Compressible Fluid," NACA TN 1800 (Feb., 1949) or NACA Rep. 958 (1950).

17. Scott, C. J. and Eckert, E. R. G.: "Heat and Mass Exchange in the Supersonic Base Region," AGARD Conference Proceedings #4, Separated Flows. Part I, 429 (May, 1966).

18. Kubota, T.: "Laminar Wake with Streamwise Pressure Gradient," GALCIT Hypersonic Research Project, Internal Memorandum No. 9 (May, 1962).

19. Lewis, J. E. and Behrens, W.: "Fluctuation Measurements in the Near Wake of a Slender Wedge at Mach 4.0 With and Without Base Injection," AIAA Paper No. 68-100 (January, 1968).

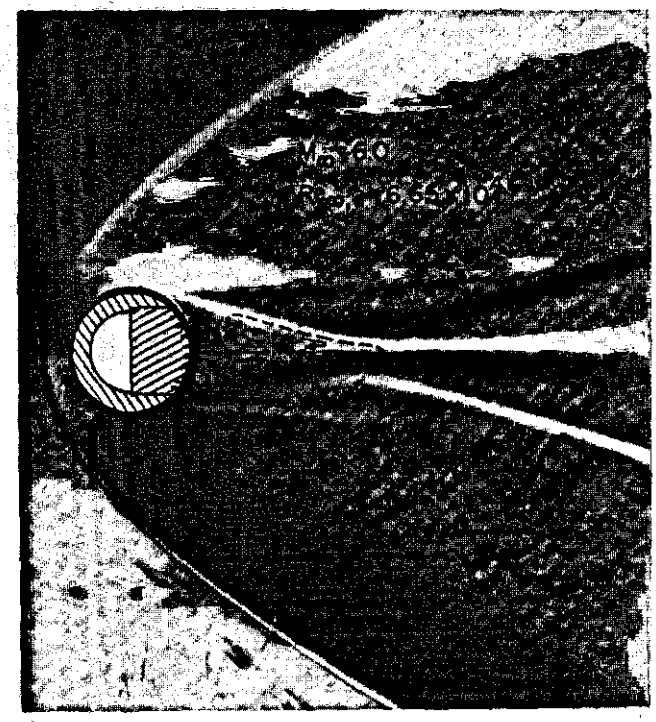

Figure 1. The Flow Field with Base Mass Addition (Schlieren photo from Reference (4))

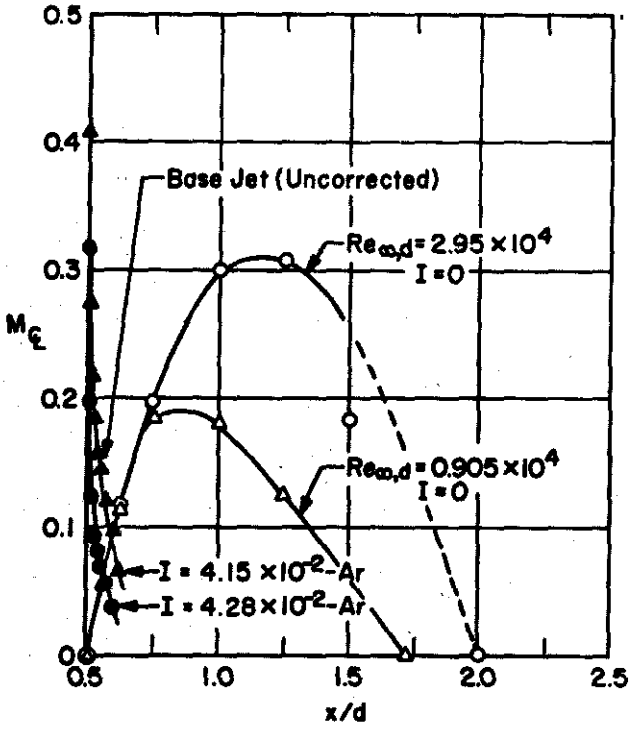

Figure 3. Axial Mach-Number Distribution in the Near Wake

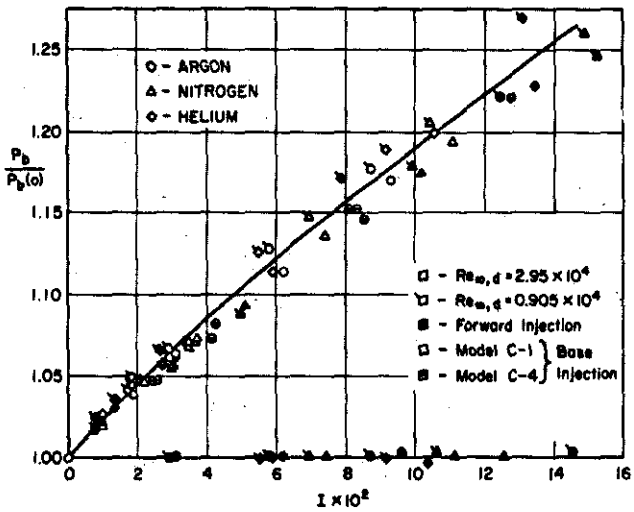

Figure 2. Variation of the Base Pressure with Mass Addition

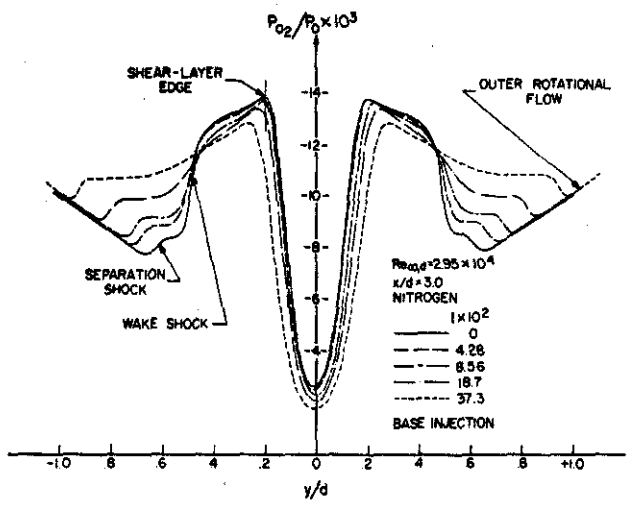

Figure 4. The Influence of Increasing Mass Addition on the Near-Wake Flow Field

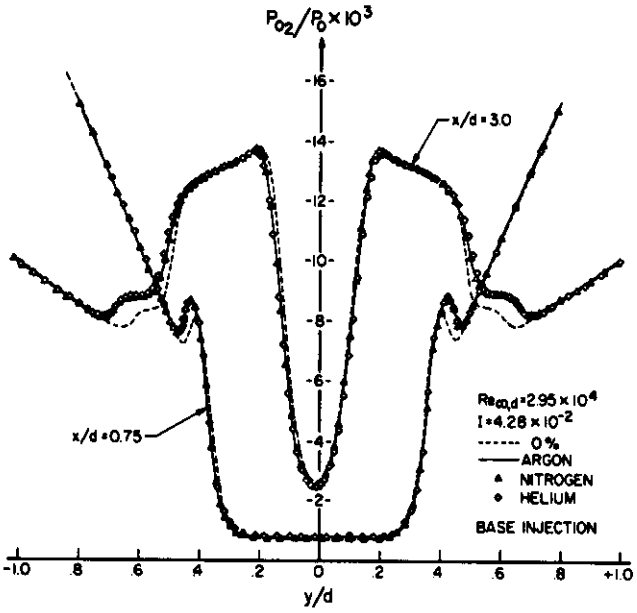

Figure 5. The Correlation of the Near-Wake Flow Field with the Mass Addition Parameter I

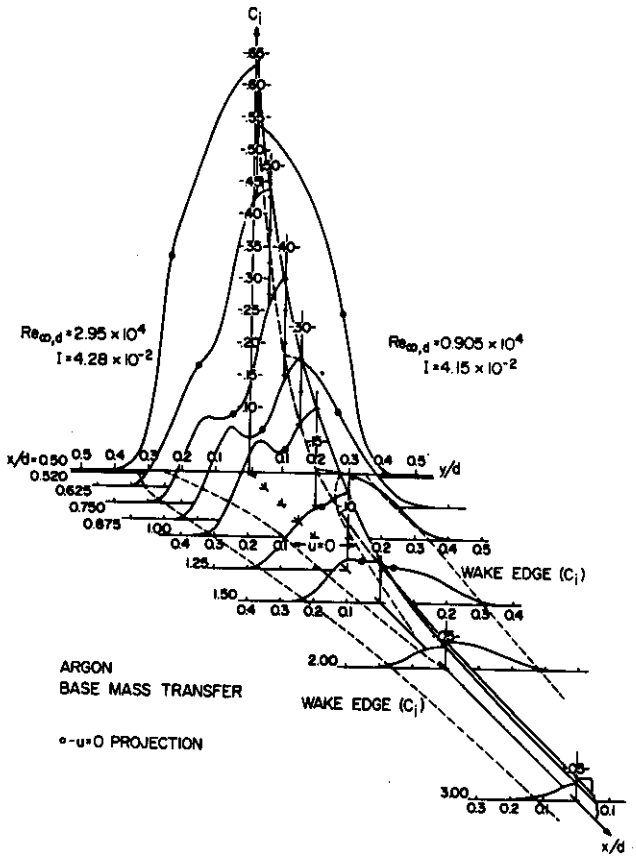

Figure 6. The Near-Wake Mass-Concentration Field for Argon Addition from the Base

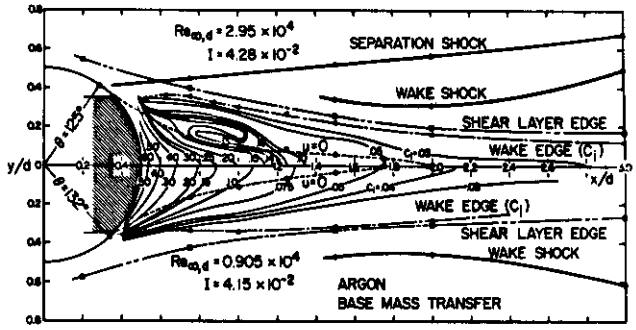

Figure 7. The Near-Wake Mass-Concentration Isogram for Argon Addition from the Base

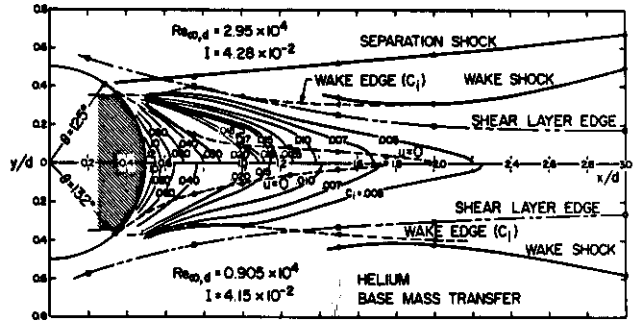

Figure 8. The Near-Wake Mass-Concentration Isogram for Helium Addition from the Base

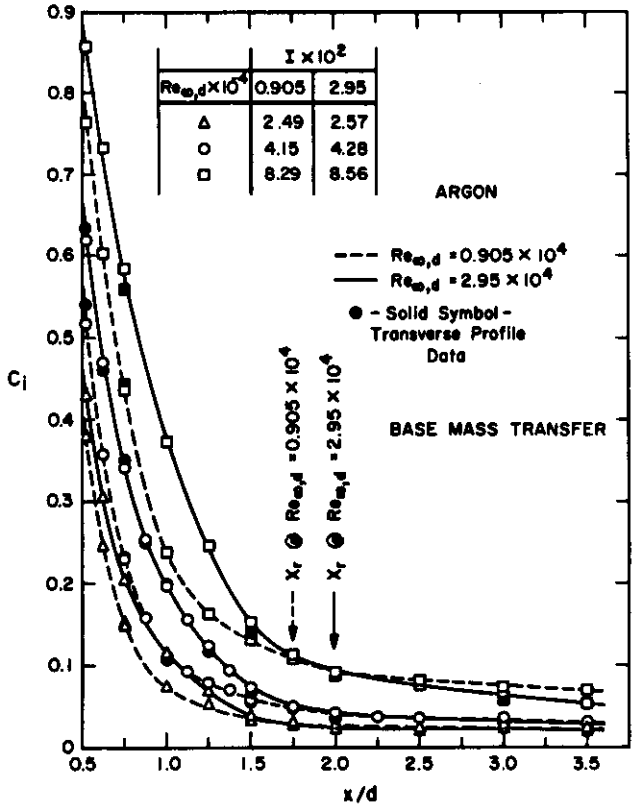

Figure 9. The Axial Distribution of Mass Concentration for Argon Addition from the Base

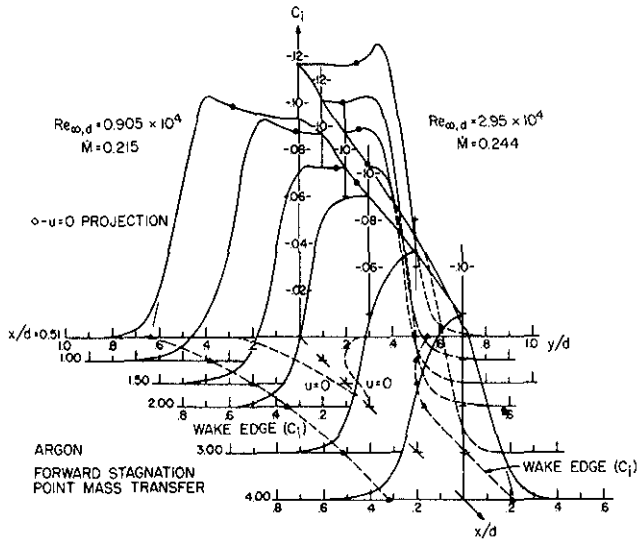

Figure 10. The Near-Wake Mass-Concentration Field for Argon Addition from the Forward Stagnation Region

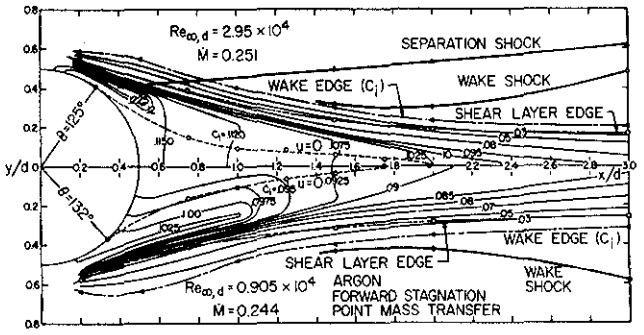

Figure 11. The Near-Wake Mass-Concentration Isogram for Argon Addition from the Forward Stagnation Region

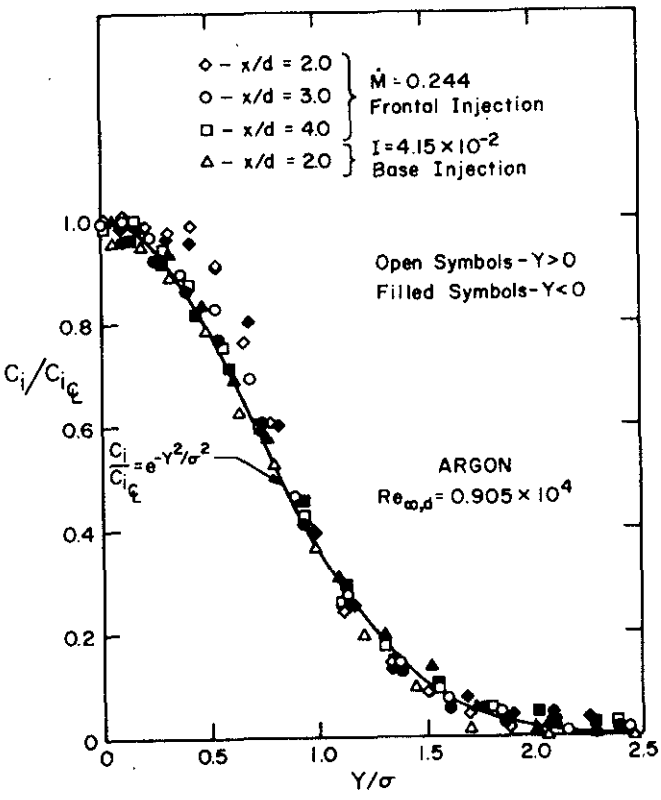

Figure 12. The Normalized Distribution of Argon Mass Concentration in the Intermediate Wake

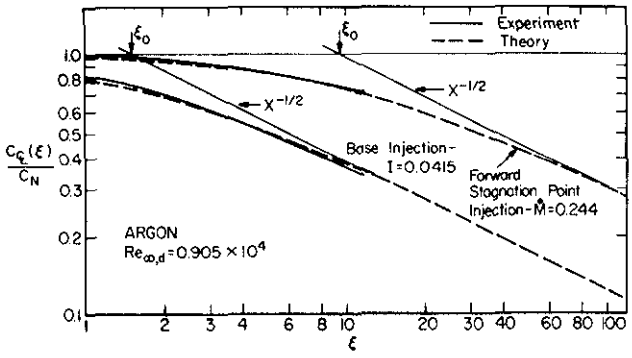

Figure 13. The Axial Mass-Concentration Distribution of Argon in the Intermediate Wake